

**Julia LIŚOŃ-KUBICA\***, **Anna TARATUTA\*\***, **Magdalena ANTONOWICZ\*\*\***,  
**Marcin BASIAGA\*\*\*\***

## **ABRASION RESISTANCE TEST OF THE MODIFIED Ti13Nb13Zr ALLOY SURFACE**

### **BADANIE ODPORNOŚCI NA ŚCIERANIE ZMODYFIKOWANEJ POWIERZCHNI STOPU Ti13Nb13Zr**

**Key words:** titanium alloys, ALD method (Atomic Layer Deposition), surface modification, bone system, antibacterial coatings.

**Abstract:** The research describes an atomic layer deposition (ALD) coating method and its application on a new generation of titanium alloy (Ti13Nb13Zr) for biomedical applications. The study aimed to assess the physicochemical properties and mechanics of a titanium alloy coated with titanium oxide (TiO<sub>2</sub>) or aluminium oxide (Al<sub>2</sub>O<sub>3</sub>) using the ALD method. The physicochemical properties of the surface coatings were evaluated through microscopic observations, potentiodynamic tests, surface wettability tests, optical profilometry scratch tests, and abrasion tests. Based on the data obtained, different physicochemical properties of the alloy with titanium nitride and titanium oxide coatings were found. Such differences were dependent on the number of cycles used and the temperature of the manufacturing process. The coatings have reduced the abrasion coefficient, thus improving the abrasion resistance of the Ti13Nb13Zr alloy, which enables their use within the skeletal system. These findings are of practical importance for applying this type of surface modification to various types of miniaturised implants used in the skeletal system.

**Słowa kluczowe:** stopy tytanu, ALD, modyfikacja powierzchni, układ kostny, powłoki antybakteryjne.

**Streszczenie:** Badania polegają na opisanu metody osadzania powłok atomowych i możliwości jej zastosowania na stopie tytanu nowej generacji do zastosowań biomedycznych. Celem pracy jest ocena wpływu właściwości fizykochemicznych i mechanicznych zmodyfikowanego stopu Ti13Nb13Zr powłoką tlenku tytanu (TiO<sub>2</sub>) oraz tlenku glinu (Al<sub>2</sub>O<sub>3</sub>) przy użyciu metody ALD. W ramach oceny własności fizykochemicznych tak powstałych powłok powierzchniowych przeprowadzono obserwacje mikroskopowe (SEM), badania potencjodynamiczne, badania zwilżalności powierzchni, profilometrię optyczną, scratch test oraz badania ścieralności powłok. Na podstawie uzyskanych danych stwierdzono zróżnicowane własności fizykochemiczne stopu z powłokami tlenku glinu oraz tlenku tytanu w zależności od zastosowanej ilości cykli oraz temperatury procesu wytwarzania. Powłoki mają obniżony współczynnik ścieralności, poprawiając tym samym odporność na ścieranie stopu Ti13Nb13Zr, co umożliwia ich zastosowanie w układzie kostnym. Uzyskana na tej podstawie wiedza ma znaczenie praktyczne dla zastosowania tego typu modyfikacji powierzchni dla różnych rodzajów zminiaturyzowanych implantów znajdujących swoje zastosowanie w układzie kostnym.

## **INTRODUCTION**

Currently, antibiotics are the main means of fighting bacterial infections. However, issues with how the

drug is administered and its effective operation have resulted in a constant search for new ways of administering them to the patient. There is also

\* ORCID: 0000-0002-0821-1756. The Silesian University of Technology, Faculty of Biomedical Engineering, Department of Biomaterials and Medical Devices Engineering, Roosevelta 40 Street, 41-800 Zabrze, Poland.

\*\* ORCID: 0000-0002-5775-1388. The Silesian University of Technology, Faculty of Biomedical Engineering, Department of Biomaterials and Medical Devices Engineering Roosevelta 40 Street, 41-800 Zabrze, Poland.

\*\*\* ORCID: 0000-0001-5755-490X. The Silesian University of Technology, Faculty of Biomedical Engineering, Department of Biomaterials and Medical Devices Engineering, Roosevelta 40 Street, 41-800 Zabrze, Poland.

\*\*\*\* ORCID: 0000-0001-5978-3861. The Silesian University of Technology, Faculty of Biomedical Engineering, Department of Biomaterials and Medical Devices Engineering, Roosevelta 40 Street, 41-800 Zabrze, Poland.

a need to develop new strategies to combat the emerging bacterial biofilms that coat the surface of implants, such as the modification of biomaterials to increase their resistance to microbial adhesion [L. 1, 2, 3]. The constantly growing need for the use of new implants in bone surgery is associated primarily with the constantly ageing society and the need to use long-term biomaterials in the case of young people. This type of material improvement consists of selecting the appropriate titanium alloy with appropriate tribological properties and high biocompatibility. The currently used titanium alloys, such as Ti6Al4V and Ti6Al7Nb, are being replaced by materials showing better biocompatibility [L. 4, 5]. Replacing elements such as vanadium or niobium allows for the so-called new generation of alloys. With the addition of Zr, Fe and Ta, these alloys gain a value close to Young's bone modulus, thus improving the biomaterial's biocompatibility. The titanium alloy currently used for research is Ti13Nb13Zr [L. 6, 7]. Tribological factors play a leading role in the loss of stability of orthopaedic endoprosthesis and determine their durability. Such tribological factors can be analysed using a number of tests, including abrasion [L. 8–11]. Previous research on the tribological properties of the Ti13Nb13Zr alloy showed it to have a low resistance to abrasive wear and low resistance to abrasive wear. Therefore, despite the many beneficial features of the Ti13Nb13Zr alloy, the key issue of increasing its abrasion resistance remains. This problem can be solved by modifying the surface; therefore, coatings are applied to improve the tested alloy's tribological properties. This enables, for example, increasing the hardness and wear resistance through friction and positively affecting the biocompatibility and corrosion resistance of metallic materials. One method that improves the titanium alloy's properties is the ALD technique. Deposition of atomic coatings is a method of nanometric processing characterising the coatings' high quality. The basic process comes from chemical vapour deposition (CVD); however, these methods have key differences. The ALD method is used by applying more reactive compounds than in CVD because each of the precursors provided is separate during the process in the working chamber, and in between individual dosages, the chamber is rinsed with an inert gas (e.g. nitrogen or argon). Single operations dosing each of the precursors and rinsing between them is one cycle ALD [L. 12–14]. During one cycle, the

coating grows to a thickness of about  $0.01 \div 0.3$  nm. The ALD technique allows the depositing of a wide range of films and oxides like –  $\text{Al}_2\text{O}_3$ ,  $\text{TiO}_2$ ,  $\text{ZrO}_2$ , and  $\text{ZnO}$  [L. 15, 16]. This study aimed to evaluate the tribological and physicochemical properties of  $\text{TiO}_2$  and  $\text{Al}_2\text{O}_3$  coatings deposited via the ALD method on Ti13Nb13Zr titanium alloy to find better properties.

## MATERIALS AND METHODS

Titanium alloy (Ti13Nb13Zr) samples were obtained from a bar of diameter  $d = 14$  mm and were ground and electropolished. The grinding was carried out on successively changing paper grades: 500, 1200, and 2000. Electrochemical polishing was performed by using a solution of phosphate sulphate. The coating application process was performed at  $100^\circ\text{C}$ , and 500 cycles were used. We proposed a series of tests to assess the suitability of the proposed surface modification method. For coating  $\text{TiO}_2$  the precursor was  $\text{TiCl}_4$ , and for  $\text{Al}_2\text{O}_3$  – TMA. Both coatings were covered the same way using the same parameters as above.

## POTENTIODYNAMIC METHOD

Initially, pitting corrosion resistance tests were performed using the potentiodynamic method. The reference electrode was Ag/AgCl 3M KCl, while the auxiliary was a platinum rod. The scan rate was set to 3 mV/s. Assays were carried out in a Ringer's solution of the following chemical composition: NaCl –  $8.6 \text{ g/dm}^3$ , KCl –  $0.3 \text{ g/dm}^3$ ,  $(\text{CaCl}_2, 2\text{H}_2\text{O})$  –  $0.33 \text{ g/dm}^3$ , at  $T = 37 \pm 1^\circ\text{C}$  and a pH of  $6.9 \pm 0.2$ . These tests provided and helped us to analyse the information concerning the structural characteristics of the coatings, possible defects, lack of sealing, substrate reactivity and the presence of barrier properties involving the electrolyte. Tests for pitting corrosion resistance were carried out in

**Table 1. 1X PBS solution concentrations**

Tabela 1. Stężenie roztworu 1x PBS

Chemical composition [mm]	
NaCl	137
KCl	2.7
$\text{Na}_2\text{HPO}_4$	10
$\text{KH}_2\text{PO}_4$	1.8

a saline solution (PBS). The chemical compositions of the lubricants used are shown in **Table 1**. The presence of the solutions was intended to create conditions similar to the natural conditions present in the human body. To make 1 L of PBS, 100 mL of 10x PBS was added to 900 mL of water.

## SCRATCH TEST

Mechanical tests, including the scratch test, are used to determine the scratch resistance. The test involved creating a scratch using a penetrator – a Rockwell diamond cone – with a gradual increase in the normal force loading applied to the penetrator (**Figure 1**). The tests were performed with an increased loading force from 0.03 to 30 N and using the following operating parameters: loading speed 10 N/min, table speed 1 mm/min and scratch length ~3 mm.

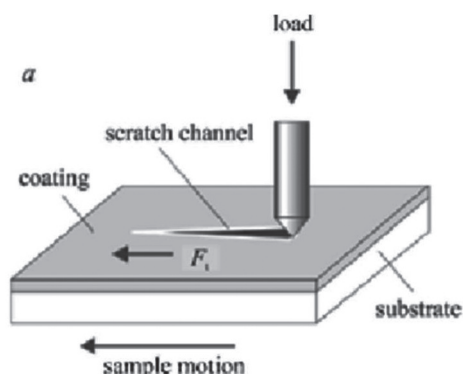


**Fig. 1. Scratch test scheme [L. 16]**

Rys. 1. Schemat scratch testu [L. 16]

## PROFILOMETRY

An optical profilometer was used to observe the  $\text{Al}_2\text{O}_3$  and  $\text{TiO}_2$  coating samples. The studies included observations of surface topography before tribological tests.

## TRIBOLOGICAL TESTING

The tribological wear test was conducted to learn about friction, wear and surface adhesion. The abrasion tests were performed using a tribometer by applying a force load of 5 N successively on all the samples, for which the following courses of the abrasion coefficient were obtained. This magnitude is connected with biomedical applications in the human body.

The tribological tests were carried out using the technical parameters in **Table 2**. A steel ball was used during these tests as a counter-sample in the friction pairs and was composed of aluminium oxide (III) –  $\text{Al}_2\text{O}_3$  with a diameter of 6 mm.

**Table 2. Technical parameters of the test**

Tabela 2. Parametry techniczne testu

Parameter	Unit	Friction pair
		Ball $\text{Al}_2\text{O}_3$ – disc Ti13Nb13Zr Steel ball – disc Ti13Nb13Zr
Load	N	5
Linear speed	cm/s	2.83
Cycle	–	1000
Frequency	Hz	80

## SCANNING ELECTRON MICROSCOPE IMAGING

Observations were made after performing tribological tests using scanning electron microscopy (SEM) (TESCAN VEGA, TESCAN, Libusina, Czech Republic). The tests were carried out in high vacuum conditions at a voltage of 15 kV, using a BSE (backscattered) detector. The images were taken at different magnifications to allow the evaluation of the trace created during the wear trace test.

## WETTABILITY

In order to determine the wettability of the surface, the contact angle method was performed on the selected samples. In order to determine the surface wettability of the selected samples, contact angle tests were performed using the sitting drop method. Measurements of the contact angle of each surface were made using distilled water with a volume of 1.5 mm<sup>3</sup> and applying the SurfTens Universal optical goniometer (OEG) and computer software SurfTens 4.5 to analyse the recorded image of the drops. The measurements were performed at room temperature ( $T = 23 \pm 1^\circ\text{C}$ ) over 60 seconds with a sampling rate of 1 Hz. The obtained data showed the different physicochemical properties of the antibacterial films generated under surface modification.

## RESULTS

### Potentiodynamic method

The samples, after grinding and polishing with the  $\text{Al}_2\text{O}_3$  and  $\text{TiO}_2$ , the coatings were applied using ALD technology and were subjected to potentiodynamic tests of the resistance to the pitting corrosion in a saline solution (PBS). The results of potentiodynamic tests are displayed in **Figures 2** and **3** at the polarisation curves.

The values shown in **Figures 2** and **3** correspond to the corrosion potential ( $E_{\text{corr}}$ ) and current density. Analysis of the course of the sample polarisation curves indicates that higher values for the  $R_p$  polarisation resistance (indicating improved corrosion resistance) occur for Ti13Nb13Zr with a  $\text{TiO}_2$  coating.

This type of surface modification had an impact on the measurement parameters. The values of the parameters that relate to the corrosion resistance of the tested samples are summarised in **Table 3**. The values shown correspond to the corrosion potential ( $E_{\text{corr}}$ ) and polarisation resistance ( $R_p$ ) in **Figure 2**.

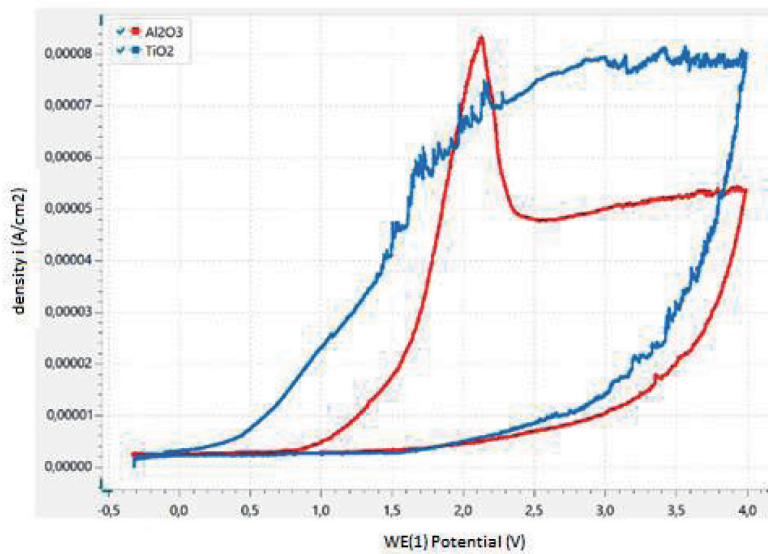


**Fig. 2.** Graphs showing the polarisation curves for the Ti13Nb13Zr alloy (with coating:  $\text{Al}_2\text{O}_3$  – red one, with coating:  $\text{TiO}_2$  – blue one)

Rys. 2. Krzywe polaryzacji dla stopu Ti13Nb13Zr (z powłoką:  $\text{Al}_2\text{O}_3$  – czerwona, z powłoką:  $\text{TiO}_2$  – niebieska)

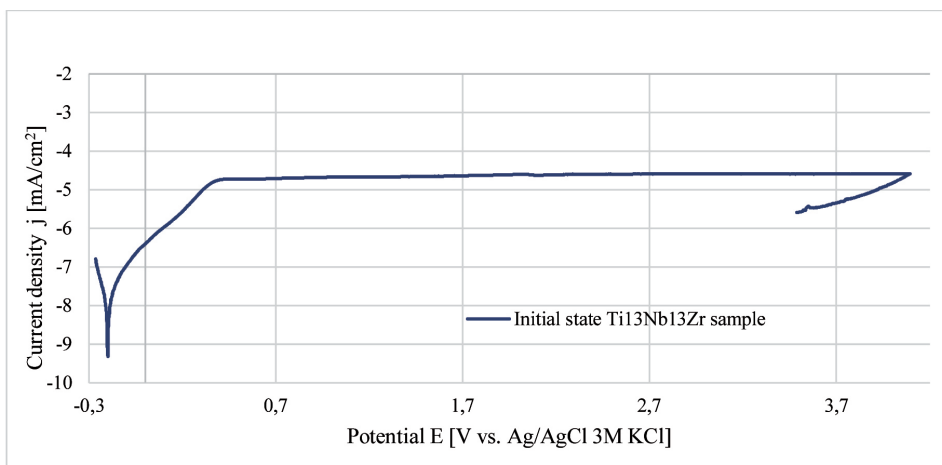


**Fig. 3.** Graphs showing the polarisation curve for the initial state Ti13Nb13Zr sample

Rys. 3. Wykresy przedstawiające krzywą polaryzacji dla próbki Ti13Nb13Zr w stanie początkowym



**Table 3. Results of potentiodynamic tests**

Tabela 3. Wyniki badań potencjodynamicznych

Sample	Polarisation data	
	E <sub>corr</sub> [V]	R <sub>p</sub> [kΩ·cm <sup>2</sup> ]
Ti13Nb13Zr	-200	1.15
Ti13Nb13Zr+Al <sub>2</sub> O <sub>3</sub>	-295	2.23
Ti13Nb13Zr+TiO <sub>2</sub>	-316	2.95

## SCRATCH TEST

In the next stage, the scratch test was conducted. On the basis of the results obtained, differences were found in the critical force values, which are a measure of adhesion. The values of the parameters corresponding to the results of the scratch test are summarised in **Table 4**.

Adhesion test data (**Table 4**) showed differences depending on the surface preparation. The sample modified by TiO<sub>2</sub> (Ti13Nb13Zr+TiO<sub>2</sub>) had the highest adhesion. The fundamental influence of the type of surface modification on the adhesion to the substrate subjected to different types of surface modification was found. Complete coating destruction (**Figures 4, 5**) was observed in every case analysed. There was no acoustic emission

signal for any of the samples, demonstrating that the bonding energy between the coating and substrate was too low. Lc3 is the force by which there is a complete layer delamination.

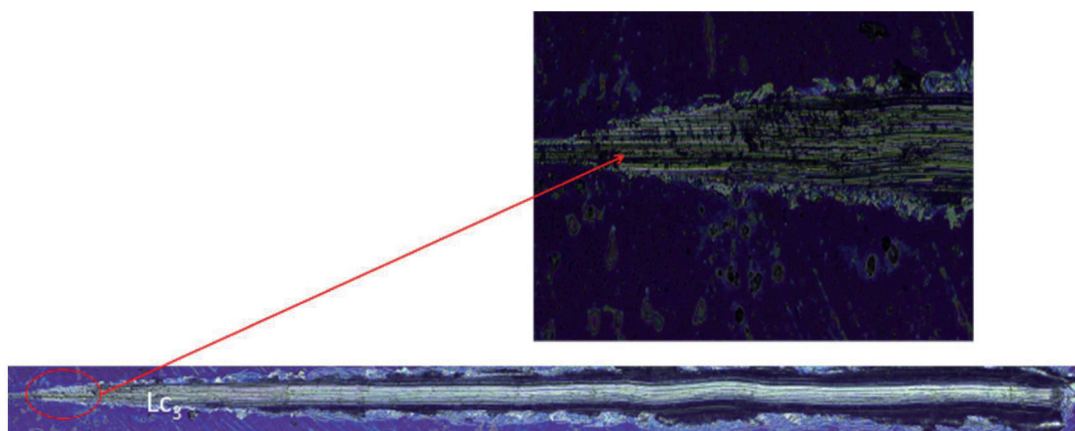
**Figure 6** shows the results of measurements of the topography of the surface prior to the tribological tests. A similar value of the Sa parameter (arithmetic mean deviation height of surface irregularities from the reference plane) was recorded on both surfaces. Ti13Nb13Zr with an Al<sub>2</sub>O<sub>3</sub> coating was Sa= 28,9273 nm, and 42,8922 nm for the Ti13Nb13Zr TiO<sub>2</sub> coating. On the other hand, observations of the surface's profile unequivocally indicated indentations and elevations of up to 100 nm in the case of the Ti13Nb13Zr with an Al<sub>2</sub>O<sub>3</sub> coating. Meanwhile, the TiO<sub>2</sub>-coated sample had deflections that reached 300 nm. The surface roughness value was twice as high for the alloy with the applied titanium oxide coating.

By applying TiO<sub>2</sub> and Al<sub>2</sub>O<sub>3</sub> coatings, the coefficient of friction ( $\mu$ ) was decreased, and the abrasion resistance improved. Following the application of the coating, the friction coefficient is decreased more for the Ti13Nb13Zr+ Al<sub>2</sub>O<sub>3</sub> coating than the Ti13Nb13Zr+TiO<sub>2</sub> coating. The average value of the coefficient friction for the tested samples is summarised in **Figures 7 and 8**.

**Table 4. Results of scratch test**

Tabela 4. Wyniki scratch testu

Method of sample surface preparation	Coating damage	Average force value F [N]
Ti13Nb13Zr+Al <sub>2</sub> O <sub>3</sub>	Complete destruction- Lc3	0.75
Ti13Nb13Zr+TiO <sub>2</sub>	Complete destruction- Lc3	1.30

**Fig. 4. Results of the adhesion tests for the Ti13Nb13Zr sample with TiO<sub>2</sub> coating (Ti13Nb13Zr +TiO<sub>2</sub>)**Rys. 4. Wyniki badań przyczepności dla próbki Ti13Nb13Zr z powłoką TiO<sub>2</sub> (Ti13Nb13Zr +TiO<sub>2</sub>)

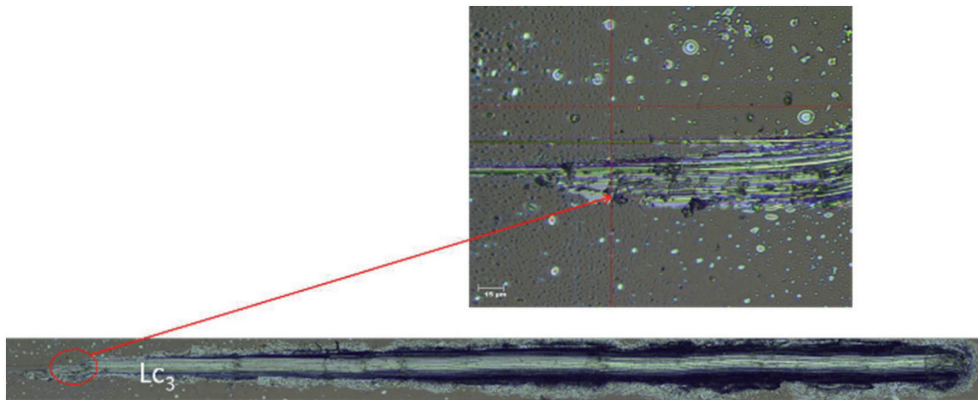


**Fig. 5. Results of the adhesion tests for a sample with  $\text{Al}_2\text{O}_3$  coating (Ti13Nb13Zr +  $\text{Al}_2\text{O}_3$ )**

Rys. 5. Wyniki badań przyczepności dla próbki z powłoką  $\text{Al}_2\text{O}_3$  (Ti13Nb13Zr +  $\text{Al}_2\text{O}_3$ )

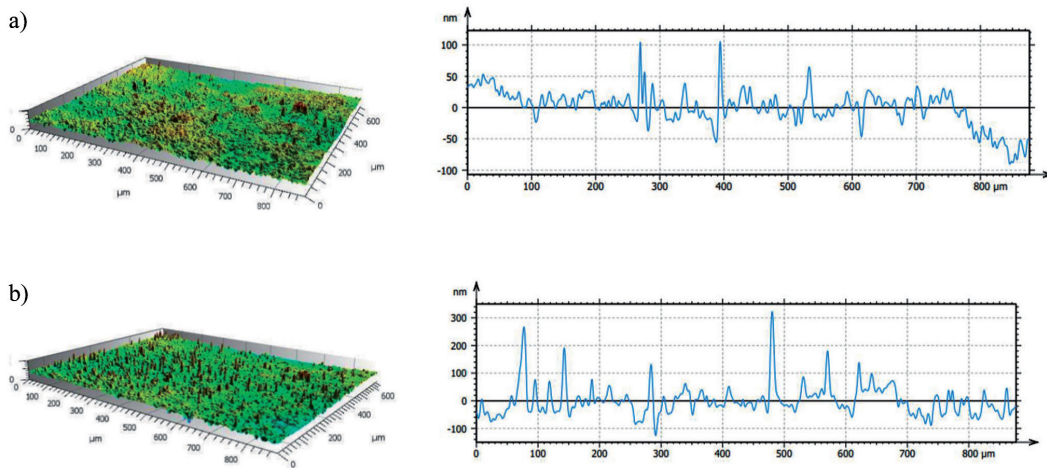


**Fig. 6. The isometric image of the surface and the profile of the surface: a) Ti13Nb13Zr with  $\text{Al}_2\text{O}_3$  coating, b) Ti13Nb13Zr with  $\text{TiO}_2$  coating**

Rys. 6. Obrazy izometryczne i profile powierzchni: a) Ti13Nb13Zr z powłoką  $\text{Al}_2\text{O}_3$ , b) Ti13Nb13Zr z powłoką  $\text{TiO}_2$

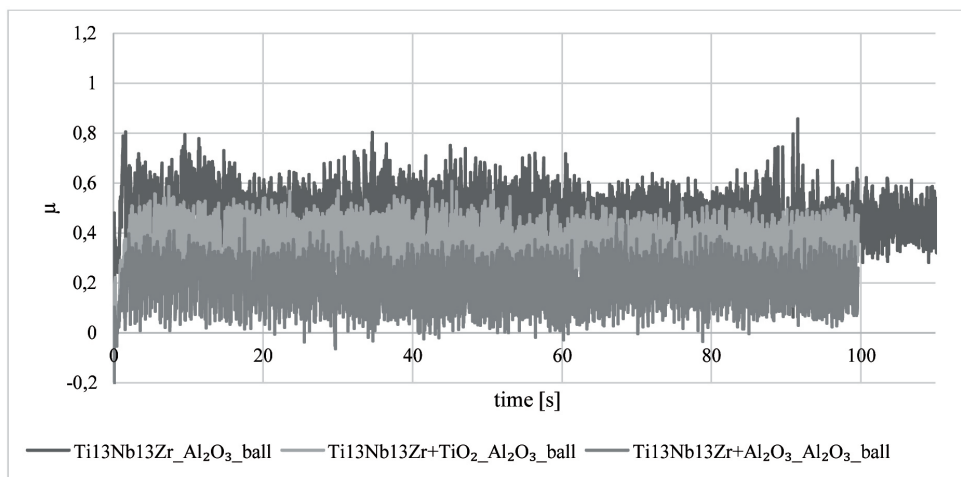


**Fig. 7. Results of tribological tests with using  $\text{Al}_2\text{O}_3$  ball**

Rys. 7. Wyniki badań tribologicznych z użyciem kulki  $\text{Al}_2\text{O}_3$

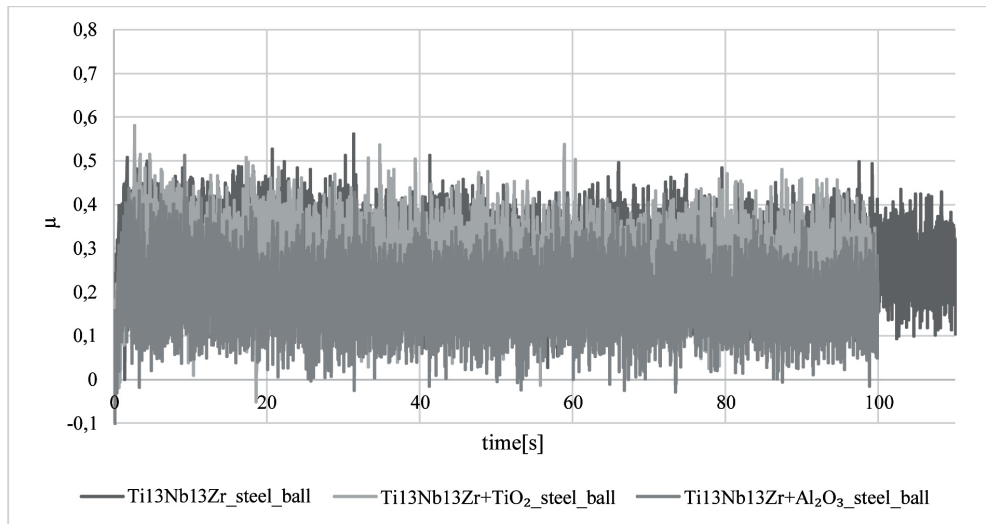


**Fig. 8. Results of tribological tests with using steel ball**

Rys. 8. Wyniki badań tribologicznych z użyciem kulki stalowej

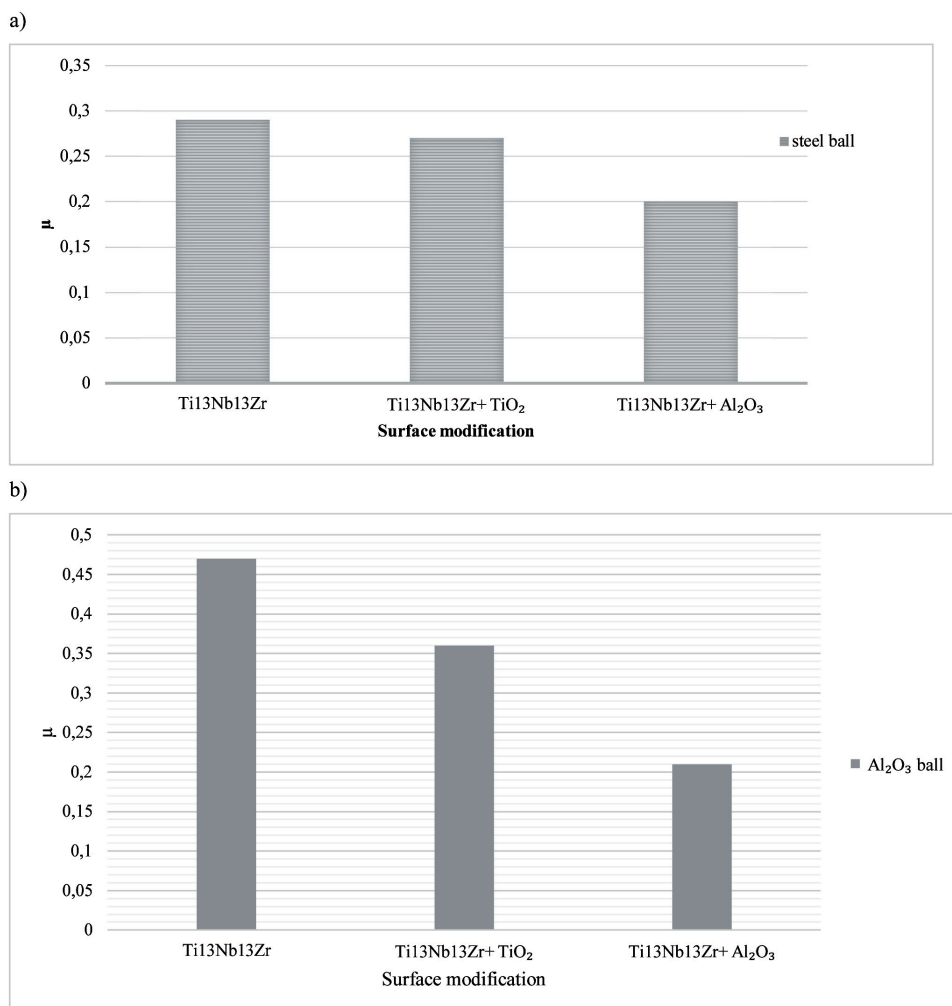


**Fig. 9. Average value of the coefficient of friction,  $\mu$ , of the Ti13Nb13Zr alloy: a) friction pair: sample-steel ball, b) friction pair: sample- $\text{Al}_2\text{O}_3$  ball**

Rys. 9. Średnia wartość współczynnika ścieralności,  $\mu$ , stopu Ti13Nb13Zr: a) para cierna: próbka-kulka stalowa, b) para cierna: próbka-kulka  $\text{Al}_2\text{O}_3$



In order to evaluate the tribological properties of the tested materials, friction tests were performed. The results obtained were summarised on a graph of the friction coefficient –  $\mu$  (**Fig. 9**) – of test elements depending on the types of materials and friction pairs. The graph shows that the best tribological characteristics were obtained for the

material combination of Ti13Nb13Zr with an  $\text{Al}_2\text{O}_3$  coating regardless of the test conditions (technically dry friction with a steel or  $\text{Al}_2\text{O}_3$  ball). Moreover, SEM observations were conducted after tribological testing, showing the abrasion trace with the  $\text{Al}_2\text{O}_3$  ball and the steel ball (**Fig. 10, 11**).

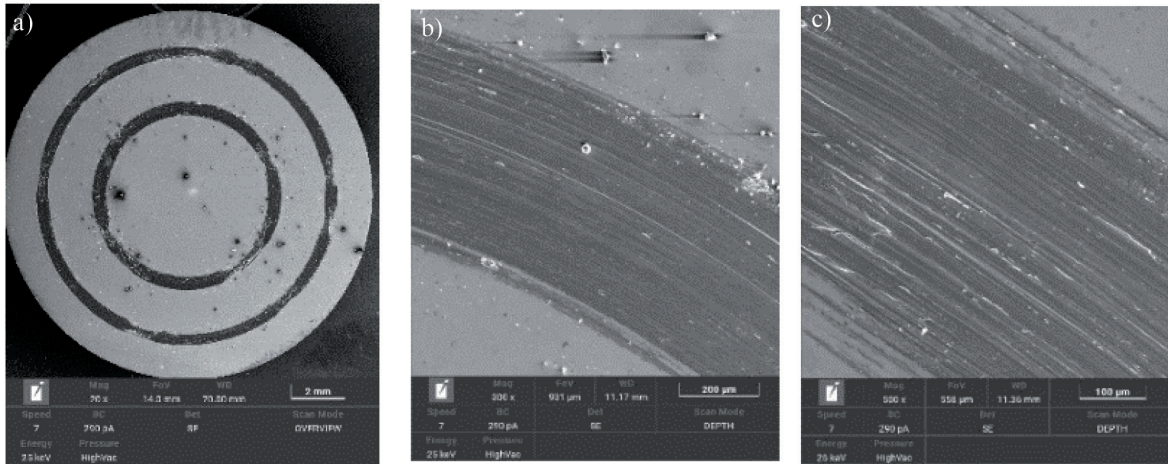


**Fig. 10.** The surface of the Ti13Nb13Zr alloy with the  $\text{Al}_2\text{O}_3$  coating after the friction pair abrasion test: Ti13Nb13Zr alloy- $\text{Al}_2\text{O}_3$  ball, SEM; area: a) 20x, b) 300x, c) 500x

Rys. 10. Powierzchnia stopu Ti13Nb13Zr z powłoką  $\text{Al}_2\text{O}_3$  po badaniu ścieralności pary cierniej: stop Ti13Nb13Zr–kulka  $\text{Al}_2\text{O}_3$ , SEM; powierzchnia: a) 20x, b) 300x, c) 500x

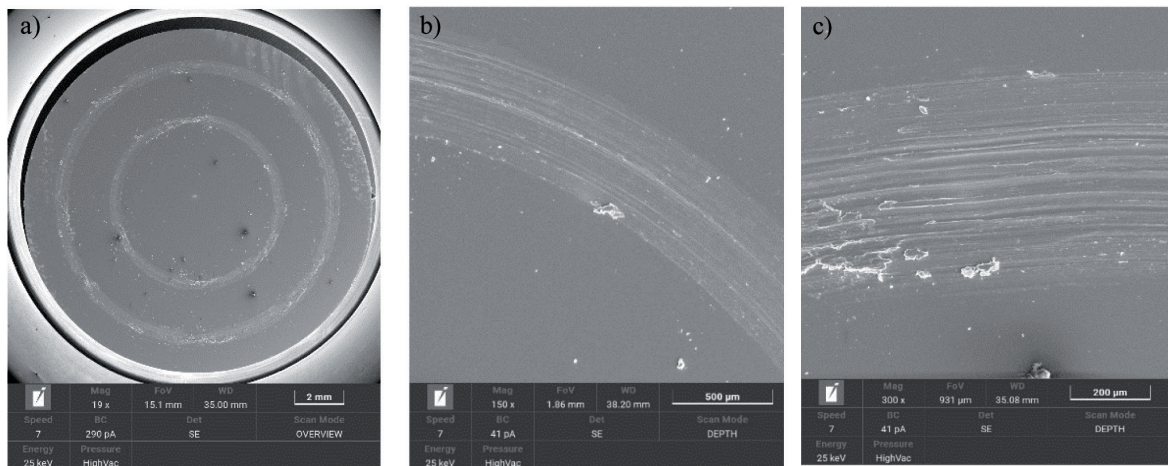


**Fig. 11.** The surface of the Ti13Nb13Zr alloy with the  $\text{TiO}_2$  coating after the friction pair abrasion test: Ti13Nb13Zr alloy-steel ball, SEM; area: a) 20x, b) 300x, c) 500x

Rys. 11. Powierzchnia stopu Ti13Nb13Zr z powłoką  $\text{TiO}_2$  po badaniu ścieralności pary cierniej: stop Ti13Nb13Zr–kulka stalowa, SEM; powierzchnia: a) 20x, b) 300x, c) 500x



## WETTABILITY

Due to the application of the coating, a change occurred in the nature of the surface and the contact angle. The average value of the contact angle for the tested samples using distilled water is summarised in **Figure 12**. The noticeable difference in the contact angle values depends on the liquid's various properties selected for the test. The 90° contact angle differentiates biomaterials by the adhered

cells being hydrophilic or hydrophobic, which influenced the appearance of the droplets during the test, as shown in **Figure 12**. In the case of an initial state of the Ti13Nb13Zr surface, the coating is not changed by the character of the surface. In the case of samples with coatings, the surface remained hydrophilic, ranging up to 90°. A hydrophilic surface is closely related to cellular proliferation and osseointegration, and such a surface remained despite the application of coatings.

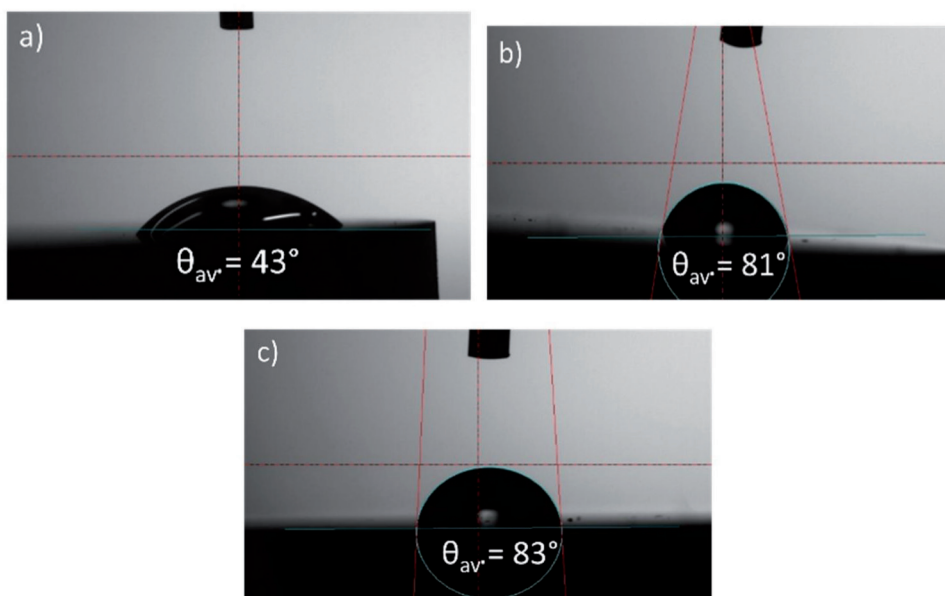


**Fig. 12** a) an example image during the measurement of wettability for the initial state of Ti13b13Zr, b) example image during wettability measurement for Ti13b13Zr alloy + TiO<sub>2</sub> coating, c) example image during wettability measurement for Ti13b13Zr alloy + Al<sub>2</sub>O<sub>3</sub> coating

Rys. 12 a) przykładowy obraz podczas pomiaru zwilżalności dla stanu wyjściowego Ti13b13Zr, b) przykładowy obraz podczas pomiaru zwilżalności dla stopu Ti13b13Zr+ powłoka TiO<sub>2</sub>, c) przykładowy obraz podczas pomiaru zwilżalności dla stopu Ti13b13Zr + powłoka Al<sub>2</sub>O<sub>3</sub>

## CONCLUSIONS

The results of this study benefit the optimisation of the ALD-based coating process of Ti13Nb13Zr alloys intended for implantation into the skeletal system. Indeed, the tribological and functional properties of the alloy's surface were improved by the methods used. The results may form the basis for further developing more detailed criteria for assessing the quality of medical devices used in the skeletal system. No clear differences were found in the pitting corrosion of the Ti13Nb13Zr alloy after applying the TiO<sub>2</sub> or Al<sub>2</sub>O<sub>3</sub> coatings, while the TiO<sub>2</sub> coating led to better potentiodynamic properties. The scratch test demonstrated that the sample coated with TiO<sub>2</sub> had the highest adhesion.

Also, the surface roughness value was twice as high for the alloy coated with TiO<sub>2</sub>. Furthermore, the TiO<sub>2</sub> coating adhered better to the substrate than the Al<sub>2</sub>O<sub>3</sub>. The coatings had reduced abrasion coefficients, which improved the abrasion resistance of the Ti13Nb13Zr alloy and would enable its use within the skeletal system. The surface was observed to have a hydrophilic nature for each variant analysed during wettability tests. Greater wettability, signified by a smaller contact angle, favours the adhesion of cells to the surface of the biomaterial. This is especially important for orthopaedic implants as it affects their integration with the host tissue. A comparison between different variants will ensure the required biocompatibility of the implants, which will minimise the risk of

postoperative complications and improve the life of patients. Cytotoxicity and biocompatibility studies should be conducted to provide a comprehensive evaluation of the performance of such layers.

### Acknowledgements

The project was funded by the Excellence Initiative – Research University programme allocated on the basis of the decision No. 32/014/SDU/10-22-16

### REFERENCES

1. Lisoń J., Taratuta A., Paszenda Z., Szindler M., Basiaga M.: Perspectives in Prevention of Biofilm for Medical Applications, *Coatings*, t. 12, 2022, pp. 1–16.
2. Bartoszewicz M., Rygiel A.: Biofilm as the basic mechanism of surgical site infection – Prevention methods in local treatment, *Pol. Surg.*, t. 8, 2006, pp. 171–178.
3. Reśliński A., Dabrowiecki S.: Evaluation of the effect of glucose on *Staphylococcus aureus* and *Escherichia coli* bio-film formation on the surface of polypropylene mesh, *Med. Dosw. Mikrobiol.*, t. 65, 2013, pp. 19–26.
4. Golvano I., Garcia I., Conde A., Tato W., Aginagalde A.: Influence of fluoride content and pH on corrosion and tribocorrosion behaviour of Ti13Nb13Zr alloy in oral environment, *J Mech Behav Biomed Mater*, t. 49, 2015, pp. 186–96.
5. Lisoń J., Taratuta A., Paszenda Z., Dwyer M., Basiaga M.: A study on the physicochemical properties of surface modified Ti13Nb13Zr alloy for skeletal implants, *Acta of Bioengineering and Biomechanics*, t. 24(1), 2022.
6. Eisenbarth E., Velten D., Müller M., Thull R., Breme J.: Biocompatibility of  $\beta$ -stabilizing elements of titanium alloys, *Biomaterials*, t. 25(26), 2004, pp. 5705–5713.
7. Bansal P., Singh G., Sidhu H.S.: Improvement of surface properties and corrosion resistance of Ti13Nb13Zr titanium alloy by plasma-sprayed HA/ZnO coatings for biomedical applications, *Materials Chemistry and Physics*, t. 257, 2021, p. 123738.
8. Madej M., Piotrowska K., Ozimina D.: Properties of diamond-like carbon coatings on the titanium alloy Ti13Nb13Zr, *Tribologia*, t. 288(6), 2019, pp. 39–46.
9. Zhang X., Zhang Y., Jin Z.: A review of the bio-tribology of medical devices, *Friction*, t. 10, 2022, pp. 4–30.
10. Zasińska K., Piątkowska A.: Ocena zużycia ściernego stopu Ti13Nb13Zr implantowanego jonami azotu przeznaczonego na elementy trące w endoprotezach ortopedycznych, *Tribologia*, t. 6, 2015, pp. 175–186.
11. Willis S.A., McGuinness E.K., Li Y., Losego M.D.: Langmuir, Re-examination of the Aqueous Stability of Atomic Coating Deposited (ALD) Amorphous Alumina ( $Al_2O_3$ ) Thin Films and the Use of a Postdeposition Air Plasma Anneal to Enhance Stability, t. 37 (49), 2021, pp. 14509–14519.
12. Boryło P., Szindler M., Szindler M., Lukaszewicz K.: Aparatura, Badania, Metody badawcze cienkich warstw wytworzonych metodą osadzania warstw atomowych, *LAB Laboratoria*, t. 24, 2019.
13. Basiaga M., Staszuk M., Walke W., Opilski Z.: Mechanical properties of atomic coating deposition (ALD)  $TiO_2$  coatings on stainless steel substrates, *Mat.-wiss. u. Werkstofftech*, t. 47, 2016, pp. 512–520.
14. Hussein M.A., Kumar A.M., Ankah N., Abdul Azeem M.: *Ceramics International*, Thermal treatment effect on the surface and in vitro corrosion characteristics of arc deposited TiN coating on Ti alloy for orthopedic applications, t. 47(16), 2021, pp. 23203–23213.
15. Basiaga M., Kajzer W., Walke W., Kajzer A., Kaczmarek M.: Evaluation of physicochemical properties of surface modified Ti6Al4V and Ti6Al7Nb alloys used for orthopedic implants, *Materials Science and Engineering: C*, t. 68, 2016, pp. 851–860.
16. Zivic F., Babic M., Adamovic D., Mitrovic S.: Influence of the surface roughness on adhesion of chrome coatings on alloy tool steel x165crmov12 Software development for coupled multiphysical problems, TR32036 View project SMART ECO system for automatic contact less washing of vehicles-SMART WASHING SYSTEMS, *Journal of the Balkan Tribological Association*, 2012.